Journal of Structural Geology, Vol. 14, No. 2, pp. 145 to 159, 1992
Printed in Great Britain

0191-8141/92 $05.00+0.00

Dislocation creep regimes in quartz aggregates

GREG HIRTH and JAN TULLIS

Department of Geological Sciences, Brown University, Providence, RI 02912, U.S.A.

(*Received* 11 *September* 1990; *accepted in revised form* 30 *June* 1991)

Abstract—Using optical and TEM microscopy we have determined that three regimes of dislocation creep occur in experimentally deformed quartz aggregates, depending on the relative rates of grain boundary migration, dislocation climb and dislocation production. Within each regime a distinctive microstructure is produced due primarily to the operation of different mechanisms of dynamic recrystallization. At lower temperatures and faster strain rates the rate of dislocation production is too great for diffusion-controlled dislocation climb to be an effective recovery mechanism. In this regime recovery is accommodated by strain-induced grain boundary migration recrystallization. With an increase in temperature or decrease in strain rate, the rate of dislocation climb becomes sufficiently rapid to accommodate recovery. In this regime dynamic recrystallization occurs by progressive subgrain rotation. With a further increase in temperature or decrease in strain rate dislocation climb remains sufficiently rapid to accommodate recovery. However, in this regime grain boundary migration is rapid, thus recrystallization occurs by both grain boundary migration and progressive subgrain rotation. The identification of the three regimes of dislocation creep may have important implications for the determination of flow law parameters and the calibration of recrystallized grain size piezometers. In addition, the identification of a particular dislocation creep regime could be useful in helping to constrain the conditions at which a given natural deformation has occurred.

INTRODUCTION

EXPERIMENTAL studies on the deformation of geologic materials have generally concentrated on either the determination of flow laws or the characterization of microstructures produced by different deformation mechanisms. Rheological data in the form of a flow law relating strain rate, temperature and stress (and possibly other thermodynamic variables) can be used to predict the mechanical behavior of rocks at geologic conditions, provided that extrapolation in temperature and strain rate can be proven valid. Flow laws have been used to provide constraints for the modelling of a wide range of geologic processes including folding (e.g. Parrish *et al.* 1976), continental rifting (e.g. Zuber *et al.* 1986) and mantle convection (e.g. Christensen & Yuen 1989). By comparing microstructures preserved in naturally deformed rocks to those produced during laboratory experiments it is possible to investigate the processes which control the mechanical behavior of the crust. For example, microstructural observations have been used to infer mechanisms responsible for the localization of strain (Aydin & Johnson 1983, Segall & Simpson 1986). Such comparisons can also provide the evidence necessary to ensure valid extrapolation of flow laws to geologic conditions (Paterson 1987).

A great deal of experimental and observational work has been performed on quartz and it has been established that there are close similarities between dislocation creep microstructures produced in the laboratory and those observed in naturally deformed rocks (Tullis *et al.* 1973, White 1976). Due to the abundance of quartz in the crust, these dislocation creep microstructures have proven to be useful for solving a wide range of problems in structural geology. For example, asymmetry of *c*-axis preferred orientations (Schmid & Casey 1986) and planar fabrics defined by recrystallized quartz grains in *S–C* mylonites (Lister & Snoke 1984) can be used to determine the kinematics of ductile shear zones. In addition, dislocation creep microstructures (such as recrystallized grain size) have been calibrated for use as paleopiezometers (e.g. Twiss 1977, Kohlstedt & Weathers 1980, Ord & Christie 1984).

Despite the large amount of previous research on quartz, there has been no comprehensive experimental study to illustrate the processes associated with dislocation creep over the entire range of conditions where it is the dominant deformation mechanism. Dislocation creep includes a strain producing mechanism (dislocation glide or, in some cases, climb) and a recovery mechanism (dislocation climb or grain boundary migration). In addition, a number of dynamic recrystallization mechanisms can accompany deformation in the dislocation creep regime (e.g. Guillope & Poirier 1979, Drury & Urai 1990). Using optical and transmission electron microscopy (TEM) we have determined that three regimes of dislocation creep occur for quartz aggregates, depending on the relative rates of dislocation production, dislocation climb and grain boundary migration (Hirth *et al.* 1989). The rates of these processes depend on the temperature, strain rate and the amount of water present during the deformation. Within each regime a distinctive microstructure is produced due primarily to the operation of different mechanisms of dynamic recrystallization.

In this paper we first illustrate the microstructures characteristic of the three regimes of dislocation creep, and illustrate the relationship between microstructural evolution and mechanical behavior in each regime. We then discuss the processes that control which regime is

dominant, and how these processes are affected by changes in temperature, strain rate and the presence of water. Finally we discuss the implications that identification of these regimes have for interpreting microstructures from naturally deformed rocks, and the extrapolation of flow laws to geologic conditions.

EXPERIMENTAL DETAILS

Starting materials

Experiments were conducted on cylinders (6.3 mm diameter, 14 mm length) cored from two orthoquartzites and a fine-grained novaculite. Heavitree quartzite has an average grain size of 210 μm, and consists of ~99% quartz with ~1% muscovite, feldspars and iron oxides. Optical observations of this quartzite show equant grains which exhibit slight undulatory extinction (Fig. 1a). TEM observations show a variable (10^{10}–10^{13} m^{-2}) density of dislocations which are sometimes tangled. This material has been used in other experimental deformation studies (e.g. Kronenberg & Tullis 1984, Mainprice & Paterson 1984). Black Hills quartzite has an average grain size of 100 μm, and consists of ~99% quartz with ~1% feldspars and iron oxides and a variable porosity (up to ~4% by volume). Optical observations of this material show equant grains with straight extinction (Fig. 1b). TEM observations show lower (10^{10}–10^{12} m^{-2}) dislocation densities than observed for the Heavitree quartzite. Black Hills quartzite has also been used in other experimental deformation studies (Tullis *et al.* 1973, Mainprice & Paterson 1984, Dell'Angelo & Tullis 1989). The fine-grained novaculite we used is of unknown origin. It has an average grain size of 2 μm and consists of ~99% quartz with ~1% impurities. TEM observations show equant grains with equilibrium textures and low (between 0 and 5 dislocations per grain) dislocation density (Fig. 1c).

Experimental procedures

The cores were jacketed in a 250 μm thick sleeve of Ag or Pt, then mechanically sealed (either 'as is' or with 0.17 ± 0.01 wt% water added) using Pt end discs. Deformation experiments were conducted in axial compression at constant displacement rates of either 1.91×10^{-7} or 1.9×10^{-8} m s^{-1} (equal to average strain rates of 1.5×10^{-5} and 1.5×10^{-6} s^{-1}) in a modified Griggs-type apparatus. At temperatures of <1000°C, solid NaCl or KCl was used as the confining medium, and at temperatures ≥1000°C soft-fired pyrophyllite was used. Additional experiments were conducted at 1000°C using a eutectic mixture of KCl–NaCl melt as the confining medium, in a molten salt assembly (Green & Borch 1989) modified for a 1 inch bore pressure vessel. All experiments were conducted at a confining pressure of 1.5 ± 0.05 GPa (includes up to 100 MPa cell and piston friction inherent to the solid medium apparatus).

Samples were subjected to varying amounts of axial strain (up to a maximum of 60%, although curves in Fig. 3 are only shown out to 45%) in order to relate the microstructural evolution to the mechanical behavior. At the end of an experiment the temperature was lowered quickly (~5°C s^{-1}) to 300°C in order to quench in the microstructure, and the differential stress was lowered to ~100 MPa. The pressure was then lowered at ~30 MPa min^{-1} keeping the differential stress less than 200 MPa. The temperature was lowered to room temperature in 100°C increments when the confining pressure reached 450, 350 and 250 MPa. Differential stress vs axial strain curves were calculated using the force measured with a standard external load cell assuming that the sample remained cylindrical with no volume change. Observed sample strengths were reproducible to ±50 MPa. Differential stresses reported for experiments using solid salt as a confining medium may include up to 100 MPa piston friction inherent to the solid medium apparatus (Green & Borch 1989). Deformed samples were impregnated with epoxy, cut in half longitudinally, and several thin sections were prepared. Microstructural observations were made using a standard petrographic microscope and a Philips EM420 transmission electron microscope.

RESULTS

Experiments on both quartzite and novaculite show that three regimes of dislocation creep occur for quartz aggregates, depending on the temperature, strain rate and amount of water present during the deformation. The experimental conditions for the three dislocation creep regimes are shown on a plot of temperature vs strain rate in Fig. 2 The lines in Fig. 2 outline approximate boundaries between the regimes; we would like to emphasize that these boundaries are gradational. The data shown for samples deformed at a strain rate of 1.5×10^{-7} s^{-1} represent experimentally deformed Quadrant quartzite described previously by Tullis (1971), Ardell *et al.* (1973) and Tullis *et al.* (1973). The location of these samples in Fig. 2 was based on optical microstructures.

With the addition of a trace amount of water the transitions between the regimes are lowered by ~100°C at experimental strain rates (compare Figs. 2a & b). However, within each regime, the microstructures and mechanical behavior of samples deformed 'as is' are indistinguishable from those deformed with added water. Thus, in the section below we only describe the mechanical behavior and microstructures which characterize each regime, and do not comment specifically on the effect of water (or other experimental variables). In this section we also include some interpretative discussion in order to show how microstructural observations were used to determine the physical processes operative during deformation. Finally, we describe the relationship between microstructural evolution and mechanical behavior for each regime in order to illustrate whether the achievement of steady state flow stress

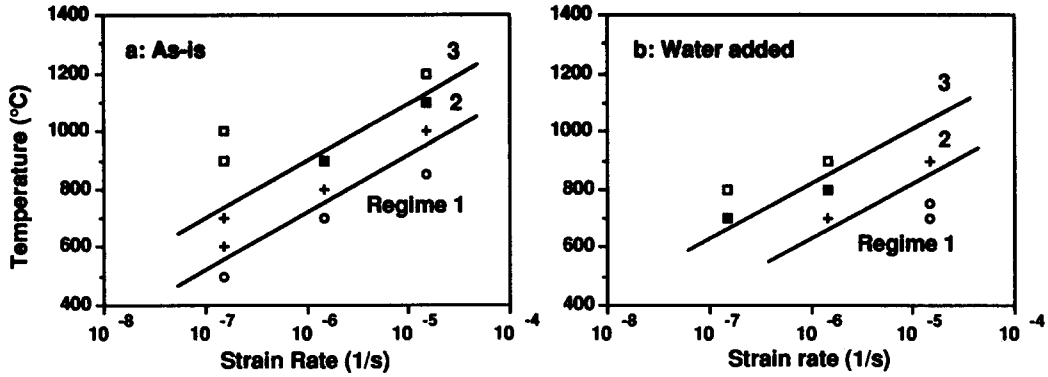

Fig. 2. Plots of temperature vs strain rate showing the location of the dislocation creep regimes for quartz aggregates deformed (a) 'as-is' and (b) with 0.17 wt% water added. The boundaries between the regimes are gradational. Open circles represent regime 1, plus symbols represent regime 2, open squares represent regime 3, and a plus inside a square represents gradational between regimes 2 and 3.

depends on the development of a steady state microstructure. Since the axial shortening geometry of the experiments limits the amount of strain and thus the amount of recrystallization possible, we also describe microstructures from samples of the fine-grained novaculite to illustrate the processes which we believe would occur in quartzite at higher strains.

Microstructural observations and interpretations

Regime 1. At lower temperatures and faster strain rates microstructural observations suggest that dislocation climb is difficult and that recovery is accommodated by grain boundary migration recrystallization. Quartzite samples deformed in this regime show the highest strengths, and they are the only ones to undergo appreciable strain weakening (Fig. 3a). However, novaculite samples deformed in regime 1 show little strain weakening (Fig. 3a).

Microstructures from quartzite samples shortened 20% show that dislocation climb is not able to accommodate recovery in regime 1. TEM observations from the cores of original grains show high densities of tangled dislocations (up to $\sim 10^{16}\,m^{-2}$) which commonly have straight segments and show no evidence for the development of subgrain boundaries (Fig. 4a). At the optical scale these grains exhibit irregular and patchy undulatory extinction (Fig. 4b). The high densities of tangled dislocations and the absence of subgrain boundaries suggest that within this regime the rate of dislocation production is greater than the rate of recovery by dislocation climb.

The onset of strain weakening shown by the quartzite at ~20% strain (Fig. 3a) corresponds to the point where recrystallization initiates at the grain boundaries. At the optical scale the recrystallized grains are too small to be resolved, and the grain boundaries appear diffuse (see arrow in Fig. 4b). TEM observations show that the mechanism of recrystallization in this regime is strain-induced grain boundary migration (Fig. 4c). We interpret the microstructure shown in Fig. 4(c) to indicate that the grains with a low dislocation density (marked with asterisks) were migrating into the work-hardened

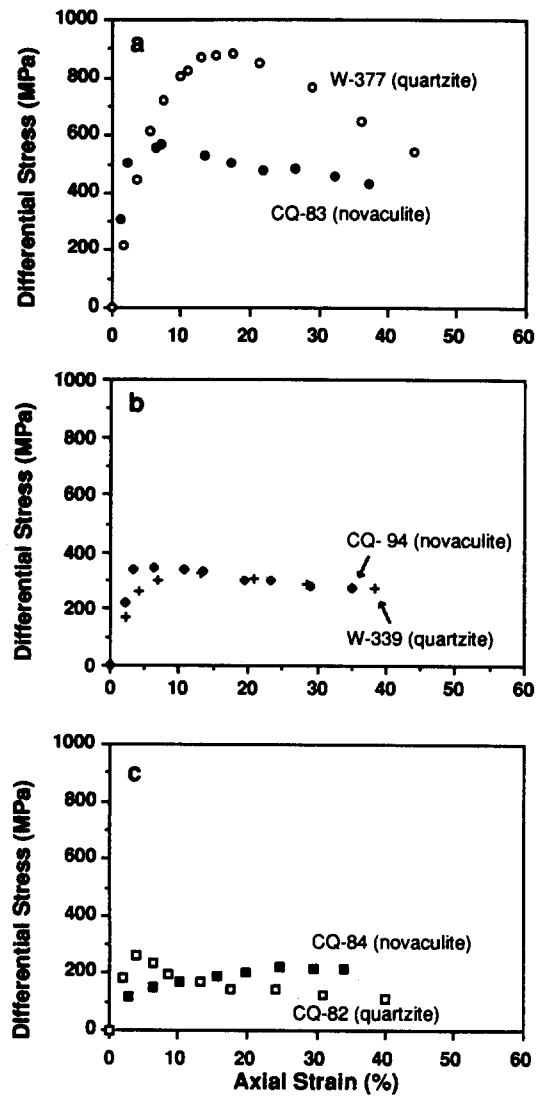

Fig. 3. Differential stress vs axial strain curves for quartzite and novaculite samples deformed in (a) regime 1, (b) regime 2 and (c) regime 3. Curves are only shown out to 45% shortening. (a) W-377, open circles: Heavitree quartzite (700°C, $10^{-6}\,s^{-1}$, 1.5 GPa, 'as-is'). CQ-83, filled circles: novaculite (700°C, $10^{-5}\,s^{-1}$, 1.5 GPa, 0.17 wt% water added). (b) W-339, pluses: Heavitree quartzite (800°C, $10^{-6}\,s^{-1}$, 1.5 GPa, 'as-is'). CQ-94, filled circles: novaculite (700°C, $10^{-6}\,s^{-1}$, 1.5 GPa, 0.17 wt% water added). (c) CQ-82, open squares: Black Hills quartzite (900°C, $10^{-6}\,s^{-1}$, 1.5 GPa, 0.17 wt% water added). CQ-84, filled squares: novaculite (900°C, $10^{-6}\,s^{-1}$, 1.5 GPa, 0.17 wt% water added).

grains. The occurrence of recrystallization-accommodated dislocation creep is well known for cold-worked metals (e.g. Sellars 1978) and has also been observed in aggregates of feldspar (Tullis & Yund 1985), aragonite (Snow & Yund 1985), olivine (Zeuch 1983) and pyroxene (Kirby & Kronenberg 1984).

While many of the recrystallized grains nucleate via a bulge mechanism at original grain boundaries (Urai *et al.* 1986), additional grains may nucleate in the grain boundary regions via a cell misorientation mechanism. TEM observations from some grain boundary regions show very small (<0.1 μm) cells and recrystallized grains within the heavily work-hardened areas of a grain (Fig. 4d). It is possible that misorientation at cell boundaries results in the formation of high-angle grain boundaries in a manner analogous to progressive subgrain rotation recrystallization. After they are nucleated, these recrystallized grains grow by strain-induced grain boundary migration.

The experiments on quartzite show that progressive recrystallization continues up to the highest strains tested (55% shortening, Fig. 3a). Optical observations of the high strain samples show inhomogeneous flattening of original grains, and extensive (20–30%) recrystallization (compare Figs. 4b & e). The recrystallized grains have a large variability in dislocation density, which is again evidence for strain-induced grain boundary migration (Fig. 4f). This microstructure also illustrates the cyclic nature of the grain boundary migration recrystallization mechanism (Sellars 1978, Tullis & Yund 1985). When a boundary migrates to create a recrystallized grain, the strain-free region is weak and able to accommodate an increment of dislocation glide. However, since climb is difficult the new grain becomes work-hardened and is eventually replaced by another grain.

The strain weakening associated with grain boundary migration recrystallization occurs because as a greater percentage of the sample becomes recrystallized, a correspondingly greater percentage of recovered (or strain-free) grains is produced (Tullis & Yund 1985). Since the recrystallized matrix is weaker than the work-hardened original grains, the strain is accommodated predominantly within the recrystallized regions. Thus after 55% shortening, many of the original grains remain equant (Fig. 4e). Similar observations have been made for feldspar aggregates which were deformed in the recrystallization-accommodated dislocation creep regime (Tullis & Yund 1985). In the high strain quartzite samples there is some evidence for the formation of subgrain boundaries (see arrow in Fig. 4f). This indicates that while grain boundary migration is the dominant accommodation mechanism, some dislocation climb does occur at the lower stresses (higher strains) in regime 1.

We would predict that a steady state flow stress in regime 1 can only be achieved after a sample is completely recrystallized. For the quartzites, many portions of original grains remain after 55% shortening (Fig. 4e). Thus, to simulate conditions where a sample becomes completely recrystallized, we conducted experiments on fine-grained novaculite. The novaculite samples are completely recrystallized after ~20% strain due to the greater surface area, and thus the greater number of nucleation sites for grain boundary bulging, in these fine-grained aggregates. TEM observations of a novaculite sample shortened 50% in regime 1 show a uniform microstructure which is the same as that observed in the highly recrystallized regions of quartzite samples. Since the stress vs strain curves for these novaculite samples show very little strain weakening, these results indicate that the achievement of mechanical steady state in regime 1 is dependent on the achievement of microstructural steady state (100% recrystallization).

Microstructural observations on the novaculite also indicate that the occurrence of strain weakening in regime 1 depends on the relationship between the original grain size and the recrystallized grain size. In the novaculite, where the recrystallized grain size is approximately the same as the original grain size, little or no strain weakening is observed (Fig. 3a). Conversely, the recrystallized grain size in the quartzite is approximately two orders of magnitude smaller than the original grain size, and the stress vs strain curves show continuous strain weakening (Fig. 3a). Similar results have been reported for torsion experiments on Ni (Sakai & Jonas 1984): strain weakening was only observed when the original grain size was greater than or equal to twice the recrystallized grain size. This relationship between weakening and recrystallized grain size is only applicable when recrystallization occurs by the grain boundary migration mechanism.

Regime 2. With an increase in temperature or a decrease in strain rate (both of which result in a decrease in flow stress), microstructural observations indicate that the rate of dislocation climb becomes sufficiently rapid to accommodate recovery. In this regime steady state flow is achieved at relatively low strain for both quartzite and novaculite (Fig. 3b).

Microstructures indicative of easy dislocation climb are apparent at both optical and TEM scales for quartzite samples shortened 30% in regime 2. The original grains exhibit a sweeping undulatory extinction, in contrast to the irregular patchy extinction observed in regime 1 (compare Figs. 5a and 4b). In addition, the original grains show optically visible subgrains and subbasal deformation lamellae. TEM observations from the cores of the original grains show that the free dislocation density is much lower than that observed for regime 1 (compare Figs. 5b and 4a), and due to the effectiveness of climb the dislocations are arranged into low energy subgrain boundaries. Within individual grains the subgrains range in diameter from ~1 to 10 μm. The subbasal deformation lamellae are defined by planar regions of higher dislocation density and elongate subgrains, consistent with previous observations on experimentally deformed quartz aggregates (Christie & Ardell 1974, 1976).

In regime 2 recrystallization occurs predominantly by

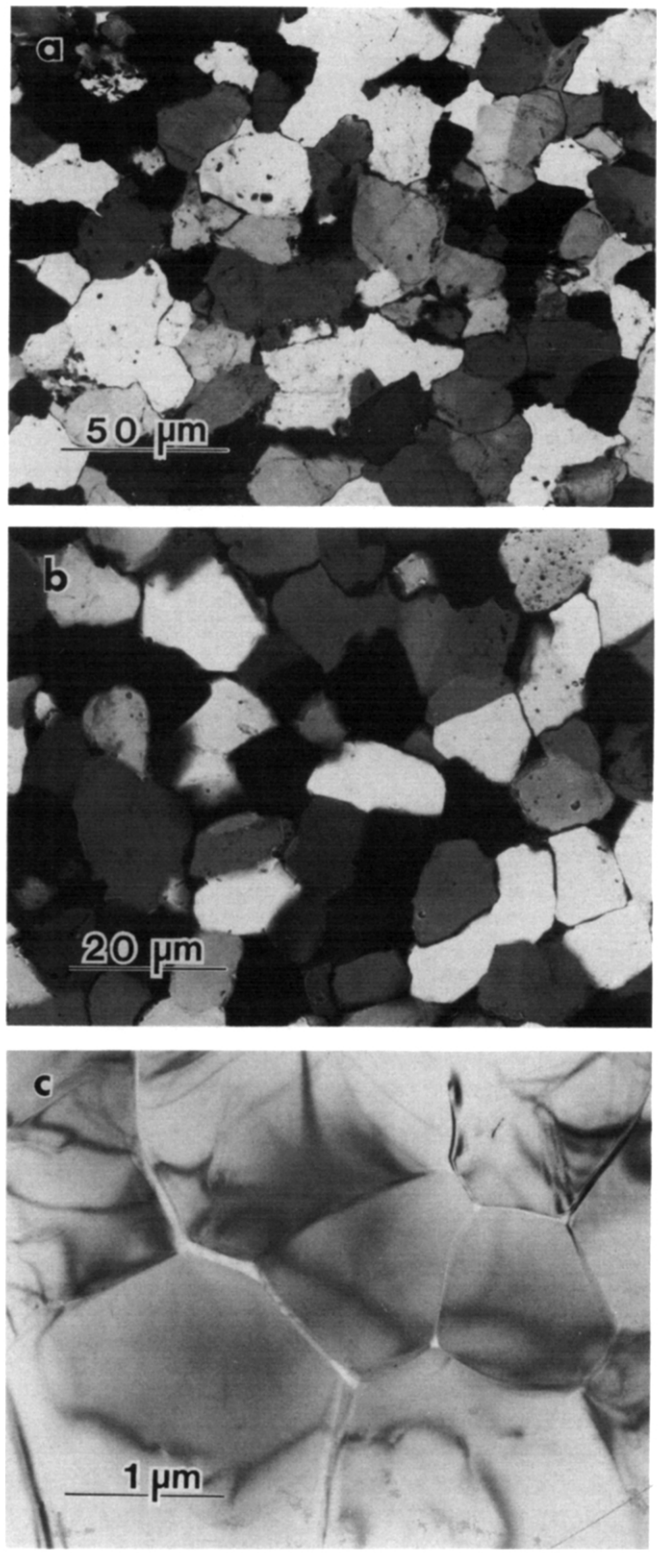

Fig. 1. Microstructures of starting materials. (a) Optical micrograph of untreated Heavitree quartzite. (b) Optical micrograph of untreated Black Hills quartzite. (c) TEM micrograph of untreated novaculite.

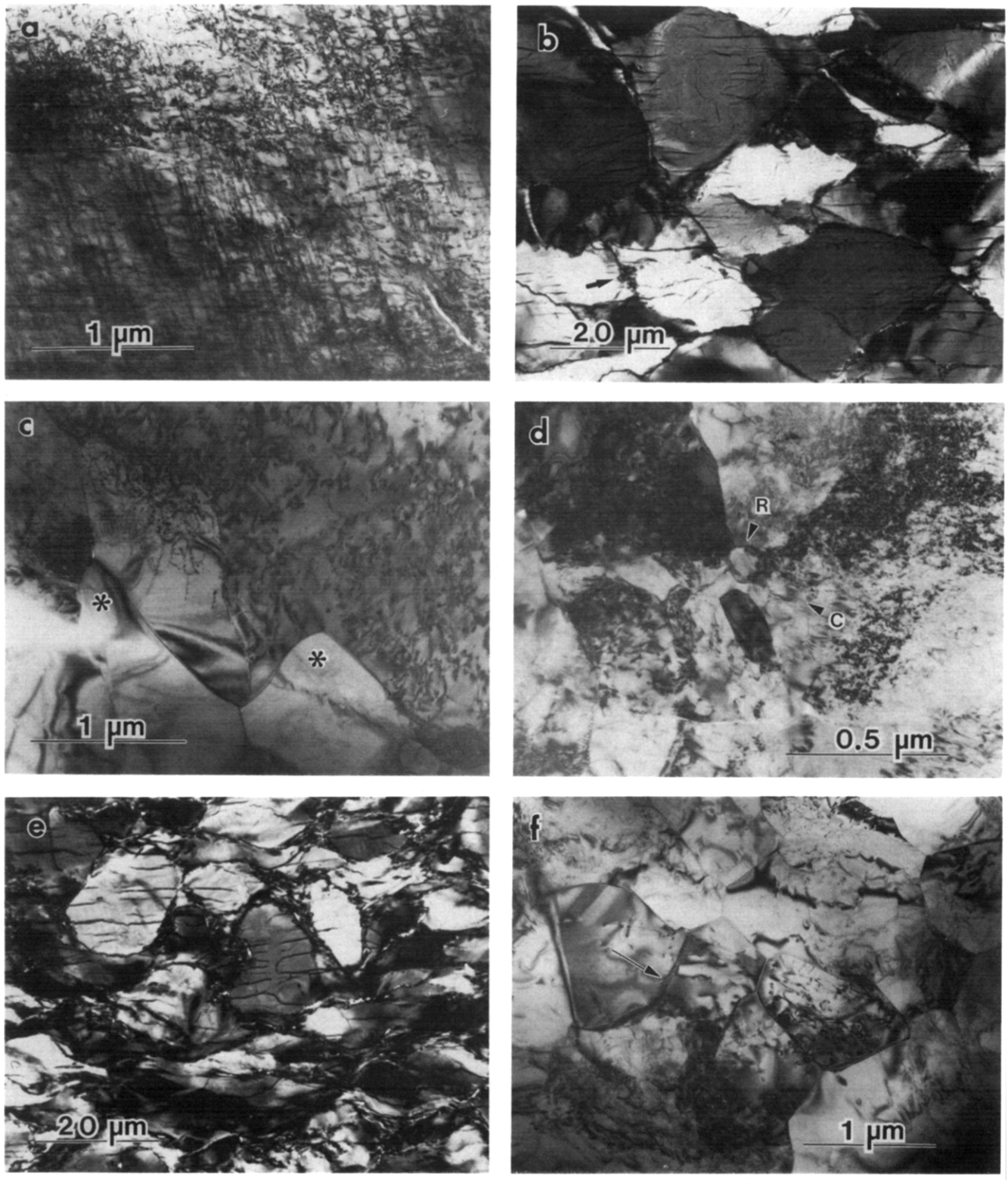

Fig. 4. Regime 1 microstructures. The shortening direction is vertical for all optical micrographs. (a) TEM micrograph of W-340 (Heavitree quartzite, 700°C, 10^{-6} s^{-1}, 1.5 GPa, 20% strain, 'as-is') from the core of an original grain with a high density of tangled and straight dislocations. (b) Optical micrograph of W-340 showing patchy undulatory extinction and diffuse grain boundaries (arrow). The horizontal microcracks formed during unloading. (c) TEM micrograph of W-340 showing initiation of grain boundary migration recrystallization. Recrystallized grains are indicated by asterisks. (d) TEM micrograph of W-340 showing grain boundary region with very small cells (c) and recrystallized grains (R). (e) Optical micrograph of W-377 (Heavitree quartzite, 700°C, 10^{-6} s^{-1}, 1.5 GPa, 58% strain, 'as-is') showing irregular patchy extinction, inhomogeneously flattened original grains and extensive grain boundary recrystallization. The horizontal microcracks formed during unloading. (f) TEM micrograph of W-348 (Black Hills quartzite, 850°C, 10^{-5} s^{-1} GPa, 45% strain, 'as-is') showing recrystallized region. The grains exhibit variable dislocation densities and some show evidence for strain-induced grain boundary migration. A few grains also show subgrain boundaries (arrow).

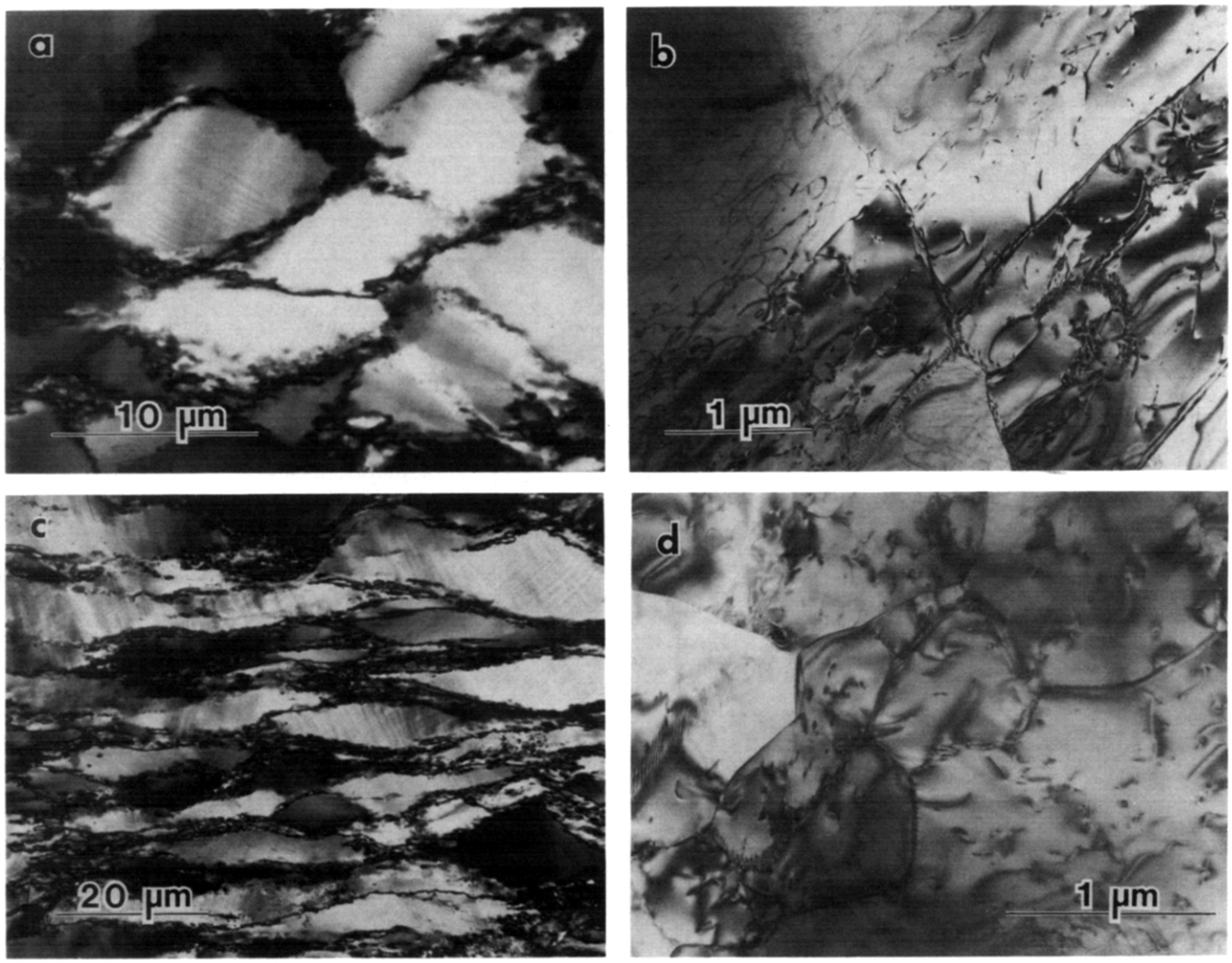

Fig. 5. Regime 2 microstructures. The shortening direction is vertical for all optical micrographs. (a) Optical micrograph of CQ-73 (Black Hills quartzite, 800°C, $10^{-6}\,s^{-1}$, 1.5 GPa, 30% strain, 'as-is') showing sweeping extinction, optically visible subgrains, deformation lamellae, and core and mantle structure. (b) TEM micrograph of CQ-73 showing low density of curved dislocations, subgrain boundaries and subgrains. (c) Optical micrograph of W-370 (Heavitree quartzite, 800°C, $10^{-6}\,s^{-1}$, 1.5 GPa, 60% strain, 'as-is') showing homogeneously flattened original grains. (d) TEM micrograph of W-370 showing recrystallized region. Recrystallized grains all have similar dislocation densities, and are bounded partly by subgrain boundaries and partly by high angle boundaries.

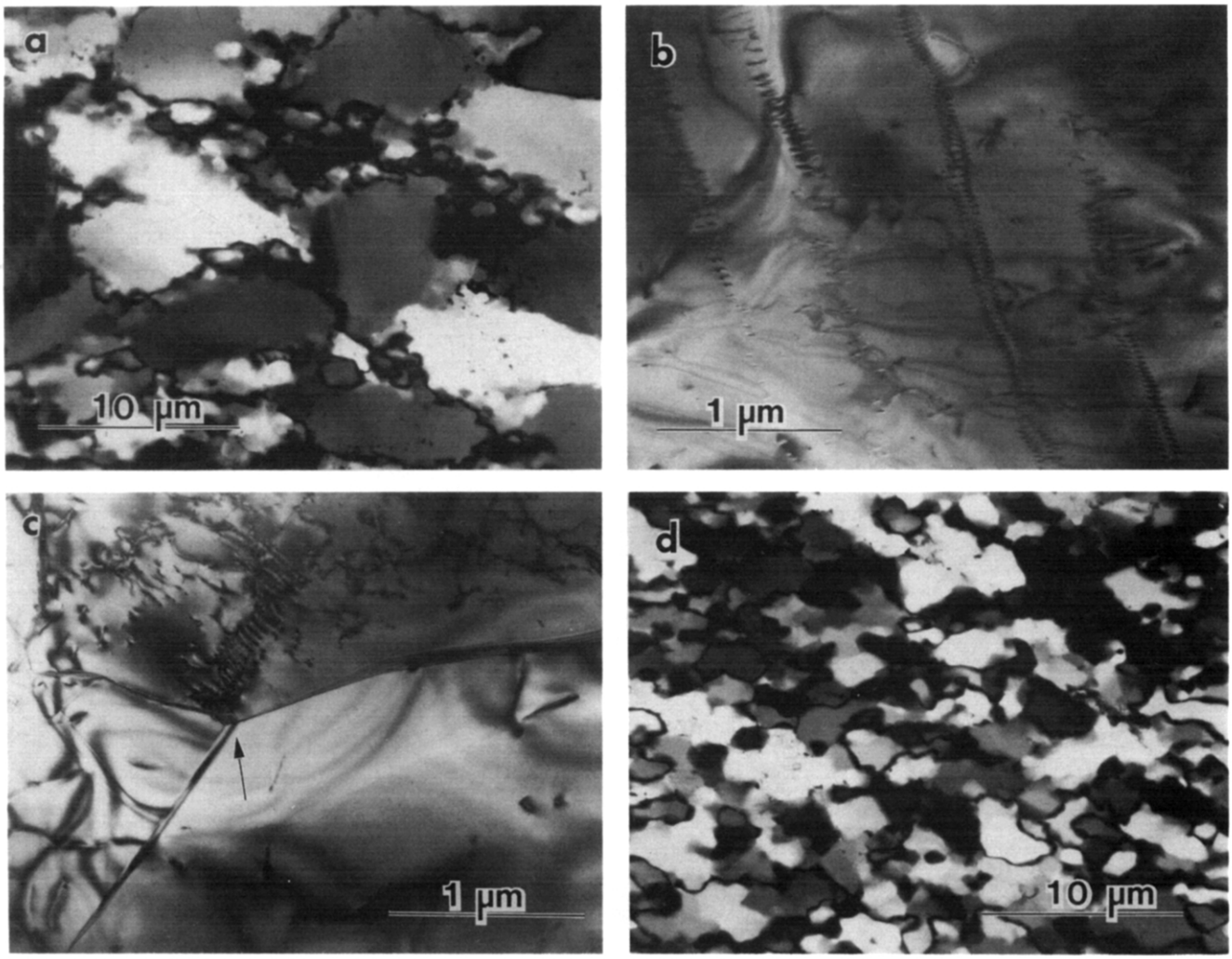

Fig. 6. Regime 3 microstructures. The shortening direction is vertical for all optical micrographs. (a) Optical micrograph of CQ-78 (Black Hills quartzite, 900°C, 10^{-6} s^{-1}, 1.5 GPa, 36% strain, 0.17 wt% water added) showing optically visible subgrains within the original grains and core and mantle structure. (b) TEM micrograph of CQ-78 showing subgrain boundaries and low dislocation density within subgrains. (c) TEM micrograph of CQ-78 showing grain boundary migrating towards subgrain boundary (arrow). (d) Optical micrograph of CQ-82 (Black Hills quartzite, 900°C, 10^{-6} s^{-1}, 1.5 GPa, 57% strain, 0.17 wt% water added) showing 100% recrystallization of original grains.

progressive subgrain rotation (i.e. 'rotation recrystallization' of Guillope & Poirier 1979). A high-angle grain boundary is formed by this mechanism when a critical number of dislocations glide and climb into a low energy subgrain boundary. This mechanism of recrystallization was first reported for experimentally deformed quartz single crystals (Hobbs 1968), and has also been observed in experimentally deformed halite (Guillope & Poirier 1979), olivine (Karato *et al.* 1982) and calcite (Schmid *et al.* 1980). Misorientation of subgrains occurs when dislocations of dominantly one sign glide and climb into the boundary, or when migrating subgrain boundaries incorporate dislocations of dominantly one sign (see fig. 7 of Urai *et al.* 1986). The amount of misorientation required to induce the transition from subgrain to high-angle grain boundary is still poorly understood, but it is clear that inhomogeneous deformation of individual grains is required (Drury & Urai 1990). Due to strain gradients which develop in the grain boundary regions, recrystallized grains initially form along the grain boundaries. This produces the distinctive core and mantle structure (White 1976) shown in Figs. 5(a) & (c). Evidence that these recrystallized grains formed by progressive subgrain rotation is best illustrated at the TEM scale. Observations from a recrystallized region of the sample shown in Fig. 5(c) indicate that the size of the recrystallized grains is similar to that of the smaller subgrains (compare Figs. 5d & b). In addition, the free dislocation density of the recrystallized grains is the same as that of the original grains from which they were formed, and individual grains may be bounded partly by high angle and partly by subgrain boundaries.

Recrystallization by the progressive misorientation of subgrains does not result in strain weakening because the recrystallized grains have about the same dislocation density as the original grains from which they formed. Thus in regime 2, the achievement of a steady state microstructure (or 100% recrystallization) is not required for the achievement of steady state flow. This is emphasized by the similarity of the stress vs strain curves for samples of novaculite and quartzite deformed in this regime.

Regime 3. With a further increase in temperature or decrease in strain rate (both of which result in a decrease in flow stress), dislocation climb remains sufficiently rapid to accommodate recovery. However, under these conditions microstructural observations indicate a significantly increased rate of grain boundary migration. In regime 3 steady state flow is again achieved at relatively low strain for both quartzite and novaculite (Fig. 3c). The strain weakening exhibited by the Black Hills quartzite is due to the reduction of locally high dislocation densities which form in response to stress concentrations around the pores when samples are taken to run conditions (Hirth & Tullis in press).

Microstructures indicating that deformation is still accommodated by dislocation climb are observed at both the TEM and optical scales in the quartzite sample shortened 36%. The original grains exhibit a core and mantle structure with optically visible subgrains that are larger than those observed for regime 2 samples (compare Figs. 6a and 5a). TEM observations from the cores of the original grains show that the free dislocation density within the subgrains is lower than that observed in regime 2 (compare Figs. 6b and 5b).

In regime 3 recrystallization occurs by both grain boundary migration and progressive subgrain rotation. A similar regime of dislocation creep has been described for polycrystalline Mg (Drury *et al.* 1984), and may be equivalent to the 'migration recrystallization' regime that Guillope & Poirier (1979) reported for single crystals of halite. Microstructural evidence for grain boundary migration is best illustrated at the TEM scale. For example, the grain boundary indicated with the arrow in Fig. 6(c) was apparently migrating in the direction of the arrow. In contrast to regime 2, notice that the recrystallized grain is significantly larger than the subgrain within the grain that it is replacing. The driving force for grain boundary migration in regime 3 may be due in part to a difference in the free dislocation density between grains. However, the grain boundaries in samples deformed in this regime are often observed to form a cusp where they intersect a subgrain boundary (see arrow on Fig. 6c). We interpret this microstructure to indicate that the energy associated with the subgrain boundaries is an important component of the driving force for grain boundary migration.

Evidence for subgrain rotation recrystallization is illustrated by the presence of a core and mantle structure within original grains (Fig. 6a). Due to concomitant grain boundary migration, it is difficult to assess how much recrystallization occurs by the subgrain rotation mechanism. However, with the operation of two recrystallization mechanisms, samples deformed in regime 3 become completely recrystallized at lower strains than samples from regime 2 or regime 1 (compare Figs. 6d, 5c and 4c).

Although recovery accommodated by grain boundary migration is significant in regime 3, the relationship between microstructural development and mechanical behavior is similar to that in regime 2. In regime 3 the achievement of a steady state flow stress is not dependent on the achievement of a steady state microstructure (at least within the resolution of our mechanical data). This is indicated by the similarity of the stress vs strain curves for quartzite and novaculite samples deformed in regime 3, and by the achievement of steady state flow stress at low strains where only a small percentage of the original grains have recrystallized. The lack of significant strain weakening can be attributed to the small difference in the dislocation density between recrystallized and original grains.

Some of the quartzite samples deformed in regime 3 exhibit small amounts (<1%) of partial melt in the grain boundary regions. However, this melt does not appear to affect the microstructural development of the quartzite. Microstructures in the novaculite samples deformed

in this regime, which contain no melt, are the same as those in the quartzite. The possible effects that the melt has on the rheological behavior are discussed below.

DISCUSSION

Transitions between dislocation creep regimes

The microstructures which we have used to identify the three regimes of dislocation creep in quartz aggregates indicate that different recovery mechanisms operate within each regime. In this section we will use these microstructural observations, in conjunction with theoretical considerations, to constrain the processes responsible for the transitions between regimes.

Transition from regime 1 *to regime* 2. The transition from regime 1 to regime 2 occurs with an increase in temperature or decrease in strain rate (Fig. 2), both of which result in a decrease in flow stress. In each case the transition occurs due to an increase in the rate of dislocation climb relative to the rate of dislocation production. The enhancement of climb is illustrated by comparing the microstructures of samples deformed in regimes 1 and 2. While the interiors of grains deformed in regime 1 exhibit high densities of tangled dislocations which commonly have straight segments (Fig. 4a), the interiors of grains deformed in regime 2 show the development of subgrain boundaries, and a lower density of free dislocations which are often curved (Fig. 5b). The enhancement of dislocation climb with increasing temperature occurs due to an increase in the rate of the diffusive process involved. The enhancement of climb with decreasing strain rate occurs because the recovery mechanism has more time to operate.

One of the diagnostic characteristics of the regime 2 microstructure is the lack of evidence for grain boundary migration. Experimental observations indicate that the velocity of grain boundary migration (V) is proportional to the driving force (F) raised to the nth power, where the proportionality constant is the grain boundary mobility (M) and n is commonly observed to be unity (Simpson & Aust 1972). In the dislocation creep regime, the predominant driving force for grain boundary migration arises from differences in strain energy which result from variations in the free dislocation density across the boundary (Poirier 1985). Grain boundary mobility is modelled as the diffusive process associated with the transport of atoms across the grain boundary (Lucke & Stuwe 1971). Thus, with a constant driving force, an increase in temperature results in an exponential increase in grain boundary velocity.

Since the transition to regime 2 occurs with increasing temperature (increasing grain boundary mobility), the lack of microstructural evidence for grain boundary migration in regime 2 indicates that the driving force for migration must be lower. A reduction in driving force in regime 2 is illustrated by the uniform dislocation density of the recrystallized and the original grains (compare Figs. 5d and 4c). The development of gradients in dislocation density is most likely to occur when limited numbers of slip systems are operative (Jessell 1986, Karato 1987). Single crystals of synthetic quartz deformed at a confining pressure of 1.5 GPa and a strain rate of $10^{-5}\,s^{-1}$ show a transition from basal slip to combined basal and prismatic slip as the temperature is increased from 600 to 700°C (Blacic 1975). Thus the transition to regime 2 may also correspond to the enhanced activity of prismatic slip, which would cause a decrease in dislocation density gradients (and thus a decrease in the driving force for grain boundary migration). Increased activity of prismatic slip in the quartzites is suggested by the more uniform flattening of original grains in regime 2 (compare Figs. 5c and 4e), which indicates that the strain is more homogeneous. In addition, the preferred orientation that develops in samples deformed in regime 2 indicates that both basal and prismatic slip systems are operative (Gleason & Tullis 1990).

Transition from regime 2 *to regime* 3. The transition from regime 2 to regime 3 also occurs with a decrease in strain rate or an increase in temperature (Fig. 2). The microstructural characteristics of regime 3 indicate that dislocation climb remains sufficiently rapid to accommodate recovery. However, microstructural observations also indicate that the rate of grain boundary migration is faster in regime 3 than it is in regime 2. The grain boundary mobility is greatest in regime 3 because it is the highest temperature regime of dislocation creep. However, the transition to regime 3 can occur with a decrease in strain rate at constant temperature (mobility), suggesting that the velocity of grain boundary migration increases due to an increase in driving force.

An increase in the driving force for grain boundary migration may arise from an increase in the relative contribution to the total energy made by the energy associated with subgrain boundaries. Microstructural observations clearly show the migration of grain boundaries preferentially into subgrain dislocation networks (Fig. 6c). We suggest that the transition to regime 3 occurs when the flow stress is low enough to allow the energy associated with subgrain (and high angle) boundaries to become a significant portion of the driving force for grain boundary migration. This process is thus similar to static grain growth, where grain boundary migration occurs as a mechanism to reduce surface energy. The relative influence of the subgrain boundaries is greater at low flow stresses because the strain energy associated with the free dislocations decreases as the dislocation density decreases. The importance of subgrain boundary energy as a driving force for grain boundary migration has also been suggested to explain the relationship between recrystallized grain size and flow stress for hot-worked metals (Derby & Ashby 1987, Derby 1991).

An alternative explanation for the transition to regime 3 is that it occurs due to a change from impurity-controlled to impurity-free grain boundary migration.

Trace amounts of soluble impurities have been shown to decrease the rate of grain boundary migration (Lucke & Stuwe 1971, Guillope & Poirier 1979). This effect is modelled as a decrease in the effective driving force which arises from a velocity-dependent tendency for impurities to accumulate along grain boundaries (dragging force). With an increase in driving force at constant temperature, or increase in temperature (mobility) at constant driving force, a transition to fast migration rates can occur if the grain boundaries break away from their impurity atmosphere (Poirier & Guillope 1979). Unfortunately, our microstructural observations are insufficient to evaluate whether the transition from regime 2 to regime 3 is a result of grain boundaries breaking away from their impurity atmosphere. However, none of our results are inconsistent with this hypothesis.

Comparison with other experimental studies

Many of the microstructures we have illustrated in this paper have been described previously for quartz aggregates experimentally deformed at similar conditions. However, some of the optical microstructures described in earlier experimental studies probably included contributions from microcracking as well as dislocation glide (e.g. Heard & Carter 1968, Ave' Lallement & Carter 1971). At temperatures lower than those shown for regime 1 in Fig. 2, a combination of optical and TEM observations shows that samples deform predominantly by cataclastic flow or develop through-going faults (Hirth & Tullis 1991). At these conditions the strain is initially accommodated by dislocation glide, but samples quickly develop high densities of tangled dislocations and work harden to very high stresses (flow stress of ~2.0 GPa at 700°C, $10^{-5}\,s^{-1}$, 1.5 GPa confining pressure), resulting in the development of distributed microcracks and brittle shear zones (Tullis *et al.* 1979, Hirth & Tullis 1991). These results indicate that the rates of climb and grain boundary migration are insufficient to accommodate the recovery.

At the optical scale, our microstructural observations are consistent with those of Tullis *et al.* (1973) for experiments conducted on Quadrant quartzite at similar conditions. The microstructures they describe are diagnostic of regime 2 (Tullis *et al.* 1973, fig. 5) and regime 3 (Tullis *et al.* 1973, fig. 6). The TEM microstructures of some of the samples from Tullis *et al.* (1973) were described by Ardell *et al.* (1973) and they are also consistent with those that we have illustrated. However, Ardell *et al.* (1973) did not report several of the diagnostic microstructures which make it possible to distinguish the different processes operative in the dislocation creep regimes. First, Ardell *et al.* (1973) claim that for samples deformed at conditions which span the range from regime 1 to regime 3, the original grains show no evidence of easy climb (recovery). We find that only in regime 1 is there no evidence of easy climb; our Figs. 5(b) and 6(b) clearly show relatively low dislocation densities and the formation of subgrain boundaries within original grains of samples deformed in regimes 2 and 3. Ardell *et al.* (1973) did not illustrate the TEM microstructures of the cores of original grains deformed at regime 2 and 3 conditions; thus we cannot evaluate the reasons for the discrepancy in interpretation. Second, Ardell *et al.* (1973) did not characterize the mechanisms of recrystallization that operated in the samples they described.

The presence of a trace amount of water has been shown to have profound effects on the microstructural development of quartzite samples deformed within the dislocation creep regimes. For example, optical microstructures produced in Heavitree quartzite deformed at 900°C, $10^{-6}\,s^{-1}$, and 1.5 GPa confining pressure are dramatically affected by the amount of water present during the experiment (Jaoul *et al.* 1984). Samples deformed after vacuum drying (~0.17 wt% water loss) show regime 1 (or possible semi-brittle cataclastic flow) microstructures; samples deformed 'as is' show regime 2 microstructures; and samples deformed with 0.4 wt% water added show regime 3 microstructures (Jaoul *et al.* 1984, fig. 3). These results are consistent with our observation that the addition of a few tenths wt% water is equivalent to increasing the temperature ~100°C at experimental strain rates (Fig. 2).

Microstructural observations described by Koch *et al.* (1989) in a study on the effect of water on the rheology of quartzite are also consistent with our results. However, they did not describe the different mechanisms of dynamic recrystallization. In addition, whereas the microstructures of their samples deformed at comparable conditions are similar to ours, the flow stresses reported by Koch *et al.* (1989) are consistently higher. For example, they report a flow stress of 940 MPa for a sample deformed 'as is' at 800°C, $10^{-6}\,s^{-1}$; at the same temperature and strain rate we observe a flow stress of ~350 MPa. However, the microstructures they show for the 940 MPa sample (fig. 11 of Koch *et al.* 1989) are almost identical to those we illustrate for the 350 MPa sample (Fig. 5d).

The discrepancy between our results and those of Koch *et al.* (1989) may be due to differences in the amount of water available during 'as is' experiments, or to the effect of confining pressure (fH_2O) on the flow stress (our experiments were conducted at 1.5 GPa while theirs were at 1.0–1.25 GPa). However, if the stresses they report are accurate, we would expect a different microstructure corresponding to the higher flow stress. Another possibility is that the discrepancy in flow stress arises due to differences in the strength of the solid confining medium used. Koch (1983) used a sleeve of Macor ceramic as the confining medium around the cold upper piston (copper was used around the sample). In the same position we have used NaCl (see Kronenberg & Tullis 1984). The strength was measured externally in both cases, but may have included a larger contribution from friction in their case.

Previous studies have shown that at experimental strain rates, high confining pressures are necessary to induce dislocation creep in quartz aggregates (Tullis *et al.* 1979, Kronenberg & Tullis 1984). The effect of

confining pressure can be illustrated by comparing the microstructural observations we have made with those of Mainprice & Paterson (1984) who deformed Heavitree quartzite at 300 MPa confining pressure. They describe regime 1 microstructures for samples deformed at 1000°C, 10^{-5} s^{-1}, with 0.3 wt% water added. At equivalent conditions (900°C, 10^{-6} s^{-1}; same regime on Fig. 2b) we observe regime 3 microstructures for samples of the same quartzite deformed at 1.5 GPa confining pressure with 0.17 wt% water added. The cause of this confining pressure effect is still not completely understood. However, it has been shown that when water is available, increasing confining pressure enhances the rates of dislocation climb and grain boundary migration (Tullis & Yund 1989). In addition, oxygen self-diffusion rates in quartz are observed to depend strongly on fH_2O (Farver & Yund 1991). Thus the effect of confining pressure on the strength of quartz aggregates may be directly related to an effect of fH_2O (Paterson 1989, Tullis & Yund 1989).

At temperatures greater than ~800°C, some of our experiments on quartzite with added water show trace amounts of grain boundary melt. Similar observations have been made by Jaoul *et al.* (1984), Mainprice & Paterson (1984) and Dell'Angelo & Tullis (1989). The grain boundary melt occurs due to the presence of trace amounts of impurity phases (micas, feldspars, iron oxides). Little or no melt was observed for experiments on the very pure novaculite samples. The presence of melt may decrease the strength of the aggregate, by reducing strain incompatibility at grain boundaries or by enhancing grain boundary diffusion creep (Jaoul *et al.* 1984, Mainprice & Paterson 1984). The presence of melt has been observed to result in a transition to diffusion creep mechanisms (e.g. Cooper & Kohlstedt 1986, Dell'Angelo *et al.* 1987), but only when the grain size is extremely fine (<10 μm). At conditions where small (~1 volume percent) amounts of melt are present in our quartzite samples, the TEM and optical scale microstructures are almost indistinguishable from those in samples of novaculite with no melt. This observation indicates that while the melt may affect the strength of the aggregate (we cannot evaluate this due to insufficient stress resolution for these experiments), dislocation creep remains the dominant deformation mechanism.

IMPLICATIONS

Interpretation of microstructures from naturally deformed quartz aggregates

Dislocation creep has been recognized as an important deformation mechanism for quartz aggregates under conditions of greenschist metamorphism or higher (e.g. White 1976, Mitra 1978). Whereas the TEM microstructures we illustrated help to constrain the processes associated with dislocation creep, it is important to emphasize that each of the dislocation creep regimes we identified has a unique optical microstructure. Thus, by comparing the optical microstructures of naturally deformed rocks to those illustrated in Figs. 4–6, it may be possible to identify the operation of a particular regime of dislocation creep. Once a positive correlation between natural and experimental microstructures has been made, it would be possible to use our results to help determine the processes which controlled the mechanical behavior of the naturally deformed aggregate. In addition, assuming that the transitions between dislocation creep regimes occur the same way in the crust as they do in our experiments (i.e. with increasing temperature, decreasing strain rate, or addition of H_2O), the identification of a particular dislocation creep regime could be useful in helping to constrain the conditions at which a given natural deformation has occurred.

The best evidence for identifying the operation of regime 1 dislocation creep is the presence of extremely patchy undulatory extinction, and a very fine recrystallized grain size. In previous studies of naturally deformed quartz aggregates, microstructures suggestive of regime 1 grain boundary migration recrystallization have been illustrated, including grain boundary bulging (e.g. White 1976, fig. 3c, Bell & Etheridge 1976, fig. 7) and small strain-free recrystallized grains (e.g. White 1976, fig. 4b). However, examples of regime 1 microstructures such as those shown in Fig. 4 appear to be rather rare. At crustal conditions where regime 1 would be expected (possibly near the brittle–ductile transition, where the crust is strongest), it is possible that the presence of water, fine grain size, and/or mica enhances pressure solution creep (e.g. Mitra 1978).

Regime 2 appears to be the only dislocation creep regime in which extremely flattened original grains develop. This microstructure is commonly observed in quartz aggregates deformed at mid-greenschist conditions (e.g. Mitra 1978, fig. 8b, Law *et al.* 1984, figs. 7b and 9b). In some cases, aspect ratios of original grains greater than 100:1 have been reported (e.g. Christie 1963). The presence of extremely flattened original grains in naturally deformed aggregates suggests that 100% recrystallization does not occur in regime 2. It is possible that the strain gradients which are required to produce recrystallized grains by the subgrain rotation mechanism are largely accommodated within the recrystallized matrix. In this case the original grains would be free to strain homogeneously after a mantle of recrystallized grains developed.

Regime 3 is characterized by the absence of highly flattened original grains in strained rocks, the large size of the recrystallized grains, and a high percentage of recrystallization. In regime 3, quartz aggregates are often 100% recrystallized, or show only remnants of the original grains (e.g. Evans & White 1984, fig. 4a). In addition, when deformation occurs non-coaxially in regime 3, the recrystallized grains often define a planar fabric which is rotated about 25° from the *C* surface (e.g. Lister & Snoke 1984, fig. 3c, Law *et al.* 1990, fig. 2). This type of fabric is probably an example of a steady state foliation (Means 1981) which represents the instan-

taneous state of strain (Lister & Snoke 1984). The development of this type of steady state foliation is favored when grain boundary migration is relatively fast (Means 1981).

Recrystallized grain size piezometry

The theoretical basis for recrystallized grain size piezometry lies in the steady state relationship between the elastic strain energy associated with free dislocations and the surface energy associated with grain boundaries (Twiss 1977). Experimental evidence indicates that grain size is more strongly dependent on stress when recrystallization occurs by grain boundary migration than when it occurs by progressive subgrain rotation (Guillope & Poirier 1979, Schmid *et al.* 1980). The importance of this difference has been recognized in the application of grain size piezometry to mantle xenoliths (Mercier 1980). On a profile of olivine recrystallized grain size vs depth, a stepped decrease in grain size is observed with increasing depth (Ave' Lallement *et al.* 1980). Mercier (1980) concluded that this discontinuity was a result of a transition from subgrain rotation to grain boundary migration recrystallization. However, we suggest that a stepped *increase* in grain size would be expected for any transition in recrystallization mechanism with increasing depth (increasing homologous temperature).

The application of recrystallized grain size piezometry to the continental crust has been based on relations calibrated using microstructures from experimentally deformed quartz aggregates (e.g. Kohlstedt & Weathers 1980, Ord & Christie 1984, Hacker *et al.* 1990). However, the importance of different mechanisms of recrystallization on the calibration of quartz piezometers has not been taken into account. Existing grain size piezometers for quartz have been determined by assuming a single log-linear relationship between differential stress and grain size (Mercier *et al.* 1977, Koch 1983). We would expect the recrystallized grain size in regimes 1 and 3 to have a greater dependence on stress than that for regime 2 if grain boundary migration recrystallization has a greater dependence on stress than subgrain rotation recrystallization. The scatter in the existing data sets is rather large, but the data from Koch (1983) do show a trend towards increasing stress dependence at the highest stresses (regime 1). It should be pointed out that the existing piezometers (Mercier *et al.* 1977, Koch 1983) were calibrated using microstructures from samples deformed with talc as a confining medium. Both the strength of talc and the problem with defining a zero stress point with the solid medium apparatus may have resulted in errors in these piezometers.

Determination of flow law parameters

The identification of the three regimes of dislocation creep has important implications for the determination of flow law parameters. If the different accommodation processes (e.g. grain boundary migration, dislocation climb) associated with dislocation creep have different activation energies and stress dependences, then a linear fit to the power law over all regimes is not expected, and extrapolation of such relationships to geologic strain rates is not warranted (see Schmid *et al.* 1980). The existing flow laws published for quartz aggregates (Parrish *et al.* 1976, Shelton & Tullis 1981, Jaoul *et al.* 1984, Kronenberg & Tullis 1984, Koch *et al.* 1989) show substantial disagreement (Kirby & Kronenberg 1987, table 3), which suggests that a single flow law for dislocation creep may not be appropriate. It is possible to fit data in which more than one process is operative with a non-linear flow law (Parrish & Gangi 1981); however, extrapolation of non-linear relations to natural conditions is again tenuous. The disagreement between the existing flow laws undoubtedly also reflects several other problems, including: use of strong confining media, resulting in poor stress resolution and difficulty in determining the 'zero stress' point; use of high differential stresses, resulting in contributions from microcracking; the presence of grain boundary melt; and the use of different and unconstrained fH_2O conditions.

Another problem associated with experimental determination of flow laws is the evaluation of whether the deformation was steady state or not. We have shown that for regime 1 mechanical steady state is only achieved after ~100% recrystallization; this never occurs for experiments on quartzites even after 50% shortening. Thus we suggest that the best way to determine steady state flow laws for quartz aggregates (especially in regime 1) would be to use fine-grained novaculites. This would make it possible to achieve steady state deformation in all three dislocation creep regimes and also to ensure that all experiments were free of grain boundary melt.

CONCLUSIONS

Using optical and TEM microscopy we have determined that three regimes of dislocation creep occur in experimentally deformed quartz aggregates, depending on the relative rates of grain boundary migration, dislocation climb and dislocation production. The rates of these processes depend on the temperature, strain rate and the amount of water present during the deformation.

In regime 1 (the lowest temperature regime) diffusion rates are too slow for dislocation climb to be an effective recovery mechanism. In this regime recovery occurs by strain-induced grain boundary migration recrystallization. The driving force for the migration arises from variations in the free dislocation density between grains. The characteristic microstructure of samples deformed in regime 1 consists of inhomogeneously flattened original grains which exhibit an irregular patchy extinction and very fine recrystallized grains along the grain boundaries. This is the only regime of dislocation creep where significant strain weakening was observed, and is thus the only regime where the achievement of a steady state

flow stress is dependent on the achievement of a steady state (completely recrystallized) microstructure.

The transition from regime 1 to regime 2 occurs due to the greater enhancement of dislocation climb relative to that of grain boundary migration with increasing temperature, decreasing strain rate, or the addition of a trace amount of water (all of which result in a decrease in flow stress). The diagnostic microstructure of samples deformed in regime 2 consists of homogeneously flattened original grains which exhibit sweeping undulatory extinction. In this regime recrystallization occurs by progressive subgrain rotation producing a distinctive core and mantle structure. This is the only regime of dislocation creep where extremely flattened original grains are produced at high strain.

The transition from regime 2 to regime 3 occurs with increasing temperature, decreasing strain rate, or the addition of a trace amount of water (again all of these changes result in a decrease in flow stress). Although the rate of dislocation climb remains sufficiently rapid to accommodate the recovery, a significant change in the microstructure is observed due to rapid grain boundary migration. The driving force for grain boundary migration in regime 3 results partly from differences in free dislocation density and partly from the energy associated with subgrain boundaries. Since both progressive subgrain rotation and grain boundary migration recrystallization occur in regime 3, samples are characterized by recrystallized grains larger than subgrains, absence of highly flattened original grains, and a high percentage of recrystallization.

The identification of the three regimes of dislocation creep may have important implications for the determination of flow law parameters and the calibration of recrystallized grain size piezometers. If the different accommodation processes (e.g. grain boundary migration, dislocation climb) associated with dislocation creep have different activation energies and stress dependences, then a linear fit to the power law over all regimes is not expected. In addition, the relationship between recrystallized grain size and stress may not be the same for the different mechanisms of dynamic recrystallization. Thus, it is possible that grain size piezometers which were calibrated using a log-linear relationship between stress and grain size may result in errors in the estimation of differential stress.

By comparing the experimentally produced microstructures to those of naturally deformed quartzites it is apparent that the three regimes of dislocation creep also occur under geologic conditions. Assuming that the transitions between the regimes occur the same way in the crust (e.g. with increasing temperature, decreasing strain rate or increasing water content), the identification of a particular regime of dislocation creep may help constrain the conditions at which a natural deformation occurred. The identification of similar regimes of dislocation creep in other common minerals (such as feldspars and pyroxenes) may help to further our understanding of the processes which control deformation in the crust.

Acknowledgements—Supported by National Science Foundation Grant EAR-8708356. We are especially grateful to R. A. Yund for the many contributions he made at all stages of this research. In addition, we thank M. Paterson for donating the Heavitree quartzite, G. Gleason, J. Farver, S. Karato and C. Teyssier for helpful discussions, and R. A. Yund, S. Getty and two anonymous reviewers for constructive comments on the manuscript.

REFERENCES

Ardell, A. J., Christie, J. M. & Tullis, J. A. 1973. Dislocation substructures in deformed quartz rocks. *Crys. Latt. Def.* **4**, 275–285.

Ave' Lallement, H. G. & Carter, N. L. 1971. Pressure dependence of quartz deformation lamellae orientations. *Am. J. Sci.* **270**, 218–235.

Ave' Lallement, H. G., Mercier, J.-C. C., Carter, N. L. & Ross, J. V. 1980. Rheology of the upper mantle: Inference from peridotite xenoliths. *Tectonophysics* **70**, 85–113.

Aydin, A. & Johnson, A. M. 1983. Analysis of faulting in porous sandstones. *J. Struct. Geol.* **5**, 19–35.

Bell, T. & Etheridge, M. A. 1976. The deformation and recrystallization of quartz in a mylonite zone, Central Australia. *Tectonophysics* **32**, 238–267.

Blacic, J. D. 1975. Plastic deformation mechanisms in quartz: The effect of water. *Tectonophysics* **27**, 271–294.

Christensen, U. R. & Yuen, D. A. 1989. Time-dependent convection with non-Newtonian viscosity. *J. geophys. Res.* **94**, 814–820.

Christie, J. M. 1963. The Moine thrust zone in the Assynt region northwest Scotland. *Univ. Calif. Publs geol. Sci.* **40**, 345–439.

Christie, J. M. & Ardell, A. J. 1974. Substructures of deformation lamellae in quartz. *Geology* **2**, 405–408.

Christie, J. M. & Ardell, A. J. 1976. Deformation structures in minerals. In: *Electron Microscopy in Mineralogy* (edited by H.-R. Wenk). Springer, New York, 373–403.

Cooper, R. F. & Kohlstedt, D. L. 1986. Rheology and structure of olivine-basalt partial melts. *J. geophys. Res.* **91**, 9315–9323.

Dell'Angelo, L. N. & Tullis, J. 1989. Fabric development in experimentally sheared quartzites. *Tectonophysics* **169**, 1–21.

Dell'Angelo, L. N., Tullis, J. & Yund, R. A. 1987. Transition from dislocation creep to melt-enhanced diffusion creep in fine-grained granitic aggregates. *Tectonophysics* **139**, 325–332.

Derby, B. 1991. The dependence of grain size on stress during dynamic recrystallization. *Acta metall. Mater.* **39**, 955–962.

Derby, B. & Ashby, M. F. 1987. On dynamic recrystallization. *Scripta metall.* **21**, 879–884.

Drury, M. R., Humphreys, F. J. & White, S. H. 1984. Large strain deformation studies using polycrystalline magnesium as a rock analogue, II, Dynamic recrystallization mechanisms at high temperatures. *Phys. Earth & Planet. Interiors* **40**, 208–222.

Drury, M. R. & Urai, J. L. 1990. Deformation-related recrystallization processes. *Tectonophysics* **172**, 235–253.

Evans, D. J. & White, S. H. 1984. Microstructural and fabric studies from the rocks of the Moine Nappe, Eriboll, NW Scotland. *J. Struct. Geol.* **6**, 369–389.

Farver, J. & Yund, R. A. 1991. Oxygen diffusion in quartz: Dependence on temperature and water fugacity. *Chem. Geol.* **90**, 55–70.

Gleason, G. & Tullis, J. 1990. The effect of dynamic recrystallization on the lattice preferred orientation of quartz aggregates. *Geol. Soc. Am. Abs. w. Prog.* **22**, A137.

Green, H. W. II & Borch, R. S. 1989. A new molten salt cell for precision stress measurement at high pressure. *Eur. J. Miner.* **1**, 213–219.

Guillope, M. & Poirier, J. P. 1979. Dynamic recrystallization during creep of single-crystalline halite: an experimental study. *J. geophys. Res.* **84**, 5557–5567.

Hacker, B. R., Yin, A., Christie, J. M. & Snoke, A. W. 1990. Differential stress, strain rate, and temperatures of mylonitization in the Ruby Mountains, Nevada: Implications for the rate and duration of uplift. *J. geophys. Res.* **95**, 8569–8580.

Heard, J. C. & Carter, N. L. 1968. Experimentally induced "natural" intragranular flow in quartz and quartzite. *Am. J. Sci.* **266**, 1–42.

Hirth, G. & Tullis, J. 1991. Mechanisms responsible for the brittle–ductile transition in experimentally deformed quartz aggregates. *Trans. Am. geophys. Un.* **72**, 286.

Hirth, G. & Tullis, J. In press. The effect of porosity on the strength of quartzite deformed in the dislocation creep regime. *Tectonophysics*.

Hirth, G., Tullis, J. & Yund, R. A. 1989. Dislocation creep regimes in quartz aggregates. *Trans. Am. geophys. Un.* **70**, 1364.

Hobbs, B. E. 1968. Recrystallization of single crystals of quartz. *Tectonophysics* **6**, 353–401.

Jaoul, O., Tullis, J. & Kronenberg, A. K. 1984. The effect of varying water contents on the creep behavior of Heavitree quartzite, *J. geophys. Res.* **89**, 4298–4312.

Jessell, M. W. 1986. Grain boundary migration and fabric development in experimentally deformed octachloropropane. *J. Struct. Geol.* **8**, 527–542.

Karato, S.-I. 1987. Seismic anisotropy due to lattice preferred orientation of minerals: Kinematic or dynamic? In: *High Pressure Research in Mineral Physics* (edited by Manghnani, M. J. & Syono, Y.), 455–471.

Karato, S.-I., Toriumi, R. & Fujii, T. 1982. Dynamic recrystallization and high-temperature rheology of olivine. In: *High Pressure Research in Geophysics* (edited by Akimoto, S. & Manghnani, M. H.), 171–189.

Kirby, S. H. & Kronenberg, A. K. 1984. Deformation of clinopyroxenite: Evidence for a transition in flow mechanisms and semibrittle behavior. *J. geophys. Res.* **89**, 3177–3192.

Kirby, S. H. & Kronenberg, A. K. 1987. Rheology of the lithosphere: selected topics. *Rev. Geophys.* **25**, 1219–1244.

Koch, P. 1983. Rheology and microstructures of experimentally deformed quartz aggregates. Unpublished Ph.D. thesis, University of California, Los Angeles.

Koch, P. S., Christie, J. M., Ord, A. & George, R. P., Jr. 1989. Effect of water on the rheology of experimentally deformed quartzite. *J. geophys. Res.* **94**, 13,975–13,996.

Kohlstedt, D. L. & Weathers, M. S. 1980. Deformation induced microstructures, paleo-piezometers and differential stresses in deeply eroded fault zones. *J. geophys. Res.* **85**, 6269–6285.

Kronenberg, A. K. & Tullis, J. 1984. Flow strengths of quartz aggregates: Grain size and pressure effects due to hydrolytic weakening. *J. geophys. Res.* **89**, 4281–4297.

Law, R. D., Knipe, R. J. & Dayan, H. 1984. Strain path partitioning within thrust sheets: Microstructural and petrofabric evidence from the Moine Thrust zone at Loch Eriboll, northwest Scotland. *J. Struct. Geol.* **6**, 477–497.

Law, R. D., Schmid, S. M. & Wheeler, J. 1990. Simple shear deformation and quartz crystallographic fabrics: A possible natural example from the Torridon area of NW Scotland. *J. Struct. Geol.* **12**, 29–45.

Lister, G. S. & Snoke, A. W. 1984. S-C mylonites. *J. Struct. Geol.* **6**, 617–638.

Lucke, K. & Stuwe, H. P. 1971. On the theory of impurity controlled grain boundary motion. *Acta metall.* **19**, 1087–1099.

Mainprice, D. H. & Paterson, M. S. 1984. Experimental studies of the role of water in the plasticity of quartzites. *J. geophys. Res.* **89**, 4257–4269.

Means, W. D. 1981. The concept of a steady state foliation. *Tectonophysics* **78**, 179–199.

Mercier, J.-C. C. 1980. Magnitude of continental lithospheric stress inferred from rheomorphic petrology. *J. geophys. Res.* **85**, 6293–6303.

Mercier, J.-C. C., Anderson, D. A. & Carter, N. L. 1977. Stress in the lithosphere: Inferences from steady-state flow of rocks. *Pure & Appl. Geophys.* **115**, 199–226.

Mitra, S. 1978. Microscopic deformation mechanisms and flow laws in quartzites within the South Mountain anticline. *J. Geol.* **86**, 129–152.

Ord, A. & Christie, J. M. 1984. Flow stresses from microstructures in mylonitic quartzites of the Moine thrust zone, Assynt area, Scotland. *J. Struct. Geol.* **6**, 639–654.

Parrish, D. K. & Gangi, A. F. 1981. A nonlinear least squares technique for determining multiple mechanism, high-temperature creep flow laws. *Am. Geophys. Un. Geophys. Monogr.* **24**, 287–298.

Parrish, D. K., Krivz, A. L. & Carter, N. L. 1976. Finite-element folds of similar geometry. *Tectonophysics* **32**, 183–207.

Paterson, M. S. 1987. Problems in the extrapolation of laboratory rheological data. *Tectonophysics* **133**, 33–43.

Paterson, M. S. 1989. The interaction of water with quartz and its influence in dislocation flow—an overview. In: *Rheology of Solids and of the Earth* (edited by Karato, S.-I. & Toriumi, M.). Oxford University Press, Oxford, 107–142.

Poirier, J.-P. 1985. *Creep of Crystals.* Cambridge University Press, Cambridge.

Poirier, J.-P. & Guillope, M. 1979. Deformation induced recrystallization of minerals. *Bull. Mineral.* **102**, 67–74.

Sakai, T. & Jonas, J. J. 1984. Dynamic recrystallization: Mechanical and microstructural considerations. *Acta metall.* **32**, 189–209.

Schmid, S. M. & Casey, M. 1986. Complete texture analysis of commonly observed quartz *c*-axis patterns. *Am. Geophys. Un. Geophys. Monogr.* **36**, 263–286.

Schmid, S. M., Paterson, M. S. & Boland, J. N. 1980. High temperature flow and dynamic recrystallization in Carrara marble. *Tectonophysics* **65**, 245–280.

Segall, P. & Simpson, C. 1986. Nucleation of ductile shear zones on dilatant fractures. *Geology* **14**, 56–59.

Sellars, C. M. 1978. Recrystallization of metals during hot deformation. *Phil. Trans. R. Soc. Lond.* **A288**, 147–158.

Shelton, G. L. & Tullis, J. 1981. Experimental flow laws for crustal rocks. *Trans. Am. geophys. Un. Tran.* **62**, 396.

Simpson, C. J. & Aust, K. T. 1972. Grain boundary migration. *Surface Sci.* **31**, 479–497.

Snow, E. & Yund, R. A. 1987. The effect of ductile deformation on the kinetics and mechanisms of the aragonite–calcite transformation. *J. metamorph. Geol.* **5**, 14–153.

Tullis, J. A. 1971. Preferred orientations in experimentally deformed quartzites. Unpublished Ph.D. thesis, University of California, Los Angeles.

Tullis, J., Christie, J. M. & Griggs, D. T. 1973. Microstructures and preferred orientations of experimentally deformed quartzites. *Bull. geol. Soc. Am.* **84**, 297–314.

Tullis, J., Shelton, G. L. & Yund, R. A. 1979. Pressure dependences of rock strengths: Implications for hydrolytic weakening. *Bull. Mineral.* **102**, 110–114.

Tullis, J. & Yund, R. A. 1985. Dynamic recrystallization of feldspar: A mechanism for ductile shear zone formation. *Geology* **13**, 238–241.

Tullis, J. & Yund, R. A. 1989. Hydrolytic weakening of quartz aggregates: The effects of water and pressure on recovery. *Geophys. Res. Lett.* **16**, 1343–1346.

Twiss, R. J. 1977. Theory and applicability of a recrystallized grain size paleopiezometer. *Pure & Appl. Geophys.* **115**, 227–244.

Urai, J. L., Means, W. D. & Lister, G. S. 1986. Dynamic recrystallization of minerals. *Am. Geophys. Un. Geophys. Monogr.* **36**, 166–199.

White, S. 1976. The effects of strain on the microstructures, fabrics, and deformation mechanisms in quartzites. *Phil. Trans. R. Soc. Lond.* **A283**, 69–86.

Zeuch, D. H. 1983. On the inter-relationship between grain size sensitive creep and dynamic recrystallization of olivine. *Tectonophysics* **93**, 151–168.

Zuber, M. T., Parmentier, E. M. & Fletcher, R. C. 1986. Extension of continental lithosphere: a model for two scales of basin and range deformation. *J. geophys. Res.* **91**, 4826–4838.